Scanning Electrochemical Microscopy. 37. Light Emission by Electrogenerated Chemiluminescence at SECM Tips and Their Application to Scanning Optical Microscopy

Fu-Ren F. Fan, David Cliffel, and Allen J. Bard*

Department of Chemistry and Biochemistry, The University of Texas at Austin, Austin, Texas 78712

Electrogenerated chemiluminescence (ECL) at a scanning electrochemical microscope (SECM) tip as the tip was moved in the vicinity of insulating and conductive substrates was studied either by ion annihilation or with a coreactant. The SECM/ECL approach curves (intensity vs tip–substrate distance, *d*) with both insulating and conducting substrates showed a decrease in ECL intensity with a decrease in *d*. Modes of operation that produced sufficiently intense and stable ECL for optical imaging are possible. The needed improvements for higher resolution and the potential application of this technique for the studies of the kinetics and mechanisms of coreactant ECL reactions are discussed.

We describe here the generation of visible light by electrogenerated chemiluminescence (ECL) at a scanning electrochemical microscope (SECM) tip as the tip is moved in the vicinity of insulating and conductive substrates. Detection of ECL emission in this apparatus has potential applications to elucidation of the mechanisms of the light-generating reactions and in scanning optical microscopy.

In the usual amperometric mode of operation of the SECM, the tip current produced by a faradaic reaction of a suitable redox species in solution is used to obtain information about the tip–substrate distance and the nature of the substrate.[1] ECL involves the generation of light at an electrode by generation of species that engage in a chemiluminescent reaction.[2] These frequently involve alternate electrogeneration of oxidized and reduced reactants, where the electron-transfer reactions between them generate excited states, or oxidation or reduction of a luminescent species in the presence of a suitable coreactant to produce emission. Both of these ECL modes have been employed in the studies that follow. While ECL is usually carried out at relatively large electrodes, Wightman and co-workers have described ECL studies at ultramicroelectrodes (UME).[3–5] These studies have
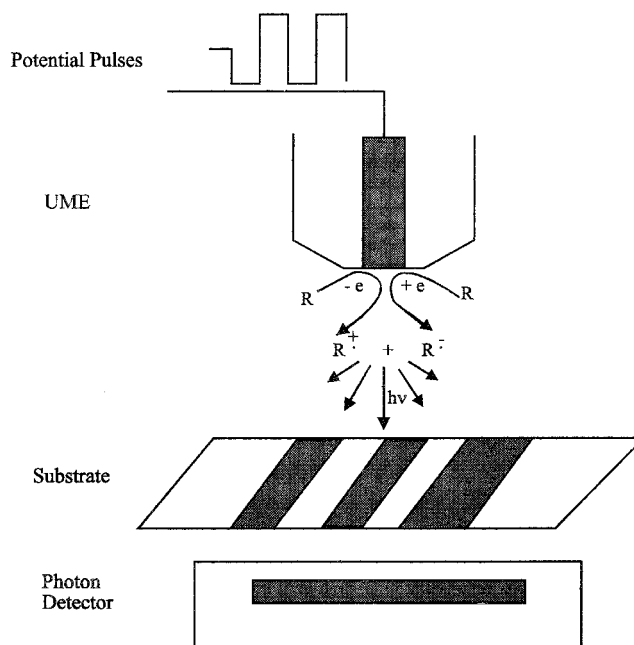

Figure 1. Schematic diagram illustrating the operating principles of ECL generation at an SECM in the alternating potential pulse mode. ECL is generated by the annihilation scheme $R^{\bullet+} + R^{\bullet-} \rightarrow 2R + h\nu$ and is detected by a PMT after attenuation by the substrate.

employed electrodes of micrometer size in bulk solution to measure the kinetics of the electron-transfer reactions and to observe individual electron-transfer events.

The basic principles of the experiment are illustrated in Figure 1. As in SECM and other forms of scanning probe microscopy,[6] the UME tip is moved and positioned with high resolution by piezoelectric elements. The electrochemical cell and bipotentiostat for controlling the UME potential and generating current are also similar to that employed in conventional SECM. In the alternating pulse mode, the ECL emission generated at the tip is detected with a photomultiplier tube or photodiode after transmission through (or reflection by) the substrate. The ECL intensity measured by the photon detector depends on the optical properties of the substrate and also on the current at the tip, which is

(1) Bard, A. J.; Fan, F.-R.; Mirkin, M. V. In *Electroanalytical Chemistry*; Bard, A. J., Ed.; Marcel Dekker: New York, 1994; Vol. 18, pp 243–373.

(2) Faulkner, L. R.; Bard, A. J. In *Electroanalytical Chemistry*; Bard, A. J., Ed.; Marcel Dekker: New York, 1977; Vol. 10, pp 1–95.

(3) Collinson, M. M.; Wightman, R. M. *Anal. Chem.* **1993,** *65,* 2576.

(4) Collinson, M. M.; Wightman, R. M. *Science* **1995,** *268,* 1883.

(5) Pastore, P.; Magno, F.; Collinson, M. M.; Wightman, R. M. *J. Electroanal. Chem.* **1995,** *397,* 19.

(6) S*canned Probe Microscopy*; Wickramasinghe, H. K., Ed.; AIP Conference Proceedings 241, American Institute of Physics: New York, 1992.

sensitive to the tip—surface distance and chemical or electro-chemical reactions at tip and substrate. Thus, by scanning the ECL probe over the surface of the substrate, images of the surface can be obtained.

The basic imaging method is similar to that employed in near-field scanning optical microscopy (NSOM),[7] in which a metal-coated quartz capillary coupled to a high-intensity laser is scanned over a surface. In such a scanning optical method the resolution obtained is governed by the diameter of the tip and in NSOM this can be as small as 50—100 nm. However, the construction of good optical tips in NSOM is challenging and there are difficulties in approaching the tip to the substrate without crashing, especially for samples immersed in liquids. Use of a metallic tip generating ECL for scanning optical microscopy has the advantage that no laser is needed and the SECM response provides feedback for positioning the tip above the substrate. In this application, however, one must be able to generate sufficient light intensities which must remain reasonably stable over the time needed to scan an image.

We describe here several different experiments describing the use of an UME to generate ECL in an SECM experiment. We demonstrate the possibility of optical imaging by this technique, although the resolution achieved is only of the order of 1 μm. We discuss the needed improvements to bring this technique to the higher resolution demonstrated in laser-driven NSOM.

EXPERIMENTAL SECTION

Tip Preparation and Apparatus. The ultramicrodisk elec-trodes were Pt disks of radius a inlaid in glass and were prepared on the basis of the procedures described previously.[1] The SECM instrument consists of a combination of electrochemical compo-nents (cell and bipotentiostat) and those used in a scanning tunneling microscope[8] for manipulating a tip at high resolution (piezoelectric drivers) and acquiring the data (computer/interface). The SECM instrument has been described in detail previously.[9,10] The ECL intensity was measured with a photo-multiplier tube (PMT, Hamamatsu R4220p or R928) and a C1230 photon-counting system (Hamamatsu Corp., Middlesex, NJ) or a home-built current-to-voltage converter followed by a voltage amplifier. The electrochemical cell contained a Pt counter electrode and a Pt quasi-reference electrode (PtQRE), which was calibrated with respect to a saturated NaCl calomel reference electrode (SSCE).

Materials. Unless indicated otherwise, Ru(bpy)$_3$$^{2+}$ (bpy = 2,2′-bipyridine) (GFS Chemicals, Powell, OH) was used as the ECL-generating molecule in all of the experiments. The chloride salt was transformed to the perchlorate form by reprecipitation from a nearly saturated aqueous solution of Ru(bpy)$_3$Cl$_2$ and LiClO$_4$. The perchlorate salt was then dried under vacuum. Tetrabutyl-ammonium fluoroborate (TBA-BF$_4$) (SACHEM, Austin, TX), recrystallized from an (acetone/ether) mixture and dried under vacuum, was used to prepare a 0.2 M supporting electrolyte solution. High-purity MeCN (Burdick & Jackson, Muskegon, MI) stored under activated 4-Å molecular sieve (J. T. Baker Inc.,
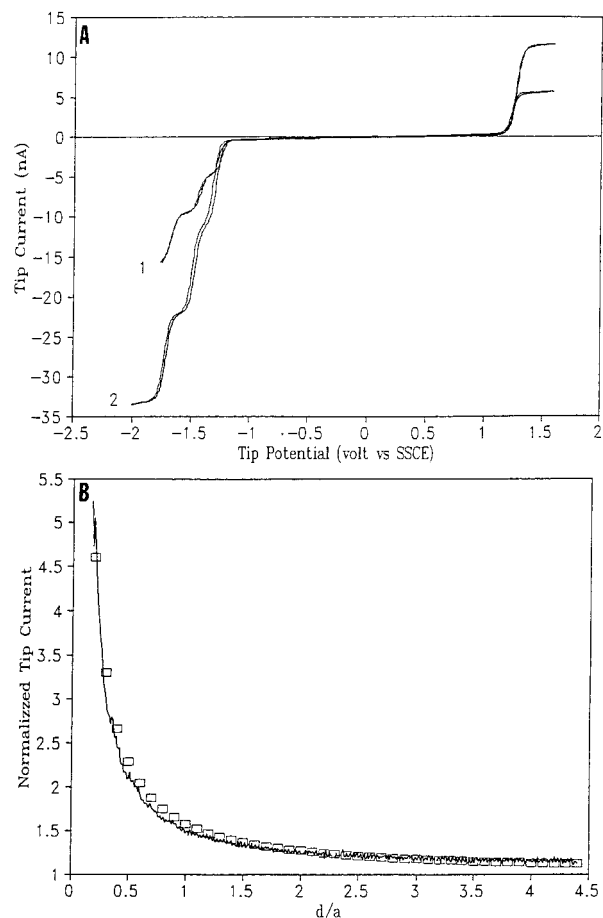
(7) Betzig, E.; Trautman, J. K.; Harris, T. D.; Weiner, J. S.; Kostelak, R. L. *Science* **1991**, *251*, 1468.
(8) Binning, G.; Rohrer, H. *Helv. Phys. Acta* **1982**, *55*, 726.
(9) Kwak, J.; Bard, A. J. *Anal. Chem.* **1989**, *61*, 1794.
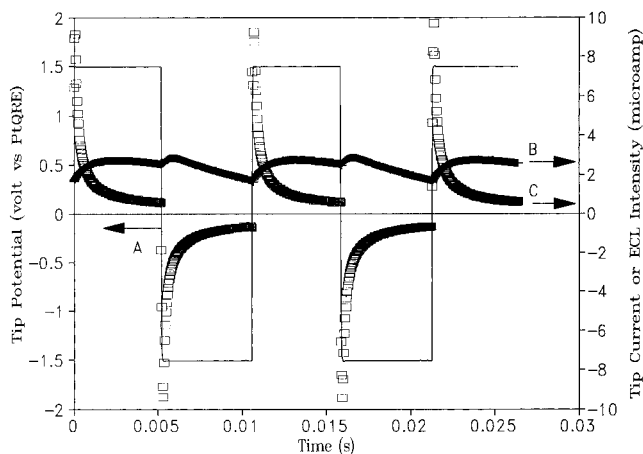(10) Fan, F.-R.; Bard, A. J. *J. Electrochem. Soc.* **1989**, *136*, 3216.

Figure 2. (A) Cyclic voltammograms of 1 mM Ru(bpy)$_3$$^{2+}$ in a 0.2 M TBA-BF$_4$/MeCN solution at a Pt microdisk electrode (a = 12.5 μm) with (curve 1) the tip far from the substrate and (curve 2) d = 0.5a. Scan rate, 5 mV/s. (B) Dependence of tip current on relative tip displacement over an ITO substrate (E_s = −0.30 V vs SSCE). The solution and tip were the same as used in (A). The tip was biased at 1.60 V vs SSCE. The tip was moved to the substrate at a speed of 0.3 μm/s. Solid curve is experimental data and squares are simulated data for a conducting substrate.

Phillipsburg, NJ) was used as the solvent. Indium tin oxide (ITO) on glass (Delta Technologies, Inc., Stillwater, MN) was degreased in trichloroethylene (Aldrich, Milwaukee, WI), washed with ethanol, and dried in air before use. Tripropylamine (TPrA) (Aldrich, Milwaukee, WI) and other chemicals were used as received. Unless indicated otherwise, all of the experiments were carried out under an argon atmosphere.

RESULTS AND DISCUSSION

Electrochemistry and SECM of Ru(bpy)$_3$$^{2+}$ over a Con-ductor. The Ru(bpy)$_3$$^{2+}$ system was used in all experiments described here. First experiments demonstrated the well-behaved electrochemistry of Ru(bpy)$_3$$^{2+}$ at the tip in SECM experiments. As shown in Figure 2A, cyclic voltammograms of Ru(bpy)$_3$$^{2+}$ in MeCN containing 0.2 M TBA-BF$_4$ as the supporting electrolyte at a Pt microdisk electrode (radius a = 12.5 μm) show three reduction waves at half-wave potentials of $E_{1/2}$ = −1.30, −1.49, and −1.73 V vs SSCE corresponding to the reduction of Ru(bpy)$_3$$^{2+}$

Figure 3. Typical wave forms of tip current (squares, curve C) and ECL intensity (pluses, curve B) accompanied by several cycles of square-wave potential of 5-ms pulse width (line, curve A). The solution contained 1 mM Ru(bpy)$_3^{2+}$ and 0.2 M TBA-BF$_4$ in MeCN. Tip and substrate ($E_s = -0.30$ V vs SSCE) were the same as used in Figure 2.

to the +1, 0, and −1 species.[11] The oxidation of Ru(bpy)$_3^{2+}$ to Ru(bpy)$_3^{3+}$ occurs at $E_{1/2} = 1.32$ V vs SSCE. As the tip was moved close to the substrate ($d = 0.5a$, where d is the separation between tip and substrate, curve 2, Figure 2A), the steady-state tip current, i_T, increased to about twice the magnitude of $i_{T,\infty}$, the steady-state tip current when the tip is far away from the substrate (curve 1, Figure 2A). This positive feedback effect is further depicted in the tip approach curve (Figure 2B), in which the tip is biased at 1.60 V vs SSCE to oxidize Ru(bpy)$_3^{2+}$ to Ru(bpy)$_3^{3+}$ while the ITO substrate is biased at −0.30 V vs SSCE to reduce Ru(bpy)$_3^{3+}$ back to Ru(bpy)$_3^{2+}$, which diffuses back to the tip. As the tip is moved toward the substrate surface, i_T increases with decreasing d, as expected from the theory.[9]

ECL Generated by Annihilation of Ru(bpy)$_3^{3+}$ and Ru(bpy)$_3^+$. By continuously applying an alternating sequence of potential pulses between 1.60 and −1.40 V vs SSCE where Ru(bpy)$_3^{3+}$ and Ru(bpy)$_3^+$ are sequentially generated at the surface of the microdisk electrode, a fairly strong and almost steady ECL intensity can be achieved through the annihilation reaction:
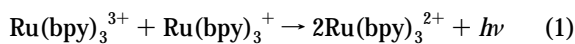
$$Ru(bpy)_3^{3+} + Ru(bpy)_3^+ \rightarrow 2Ru(bpy)_3^{2+} + h\nu \qquad (1)$$

Figure 3 shows typical wave forms of the tip current and ECL intensity accompanied by several cycles of square-wave potential of 5-ms pulse width (τ). An almost constant ECL intensity was obtained due to the electronic filtering of the light-measuring circuit, which had a time constant of ~0.5 ms. The shape of the tip current wave form was not distorted by the current-measuring circuit and followed Cottrell behavior reasonably well except in the short-time-scale region where double-layer charging was important.[12]

The ECL intensity increased monotonically with decreasing pulse width in the range of τ studied (50 μs−10 ms). It was proportional to the inverse square root of τ when τ was greater

(11) Tokel, N. E.; Bard, A. J. *J. Am. Chem. Soc.* **1972**, *94*, 2862.
(12) Bard, A. J.; Faulkner, L. R. *Electrochemical Methods: Fundamentals and Applications*; J. Wiley & Sons: New York, 1980; Chapter 5.
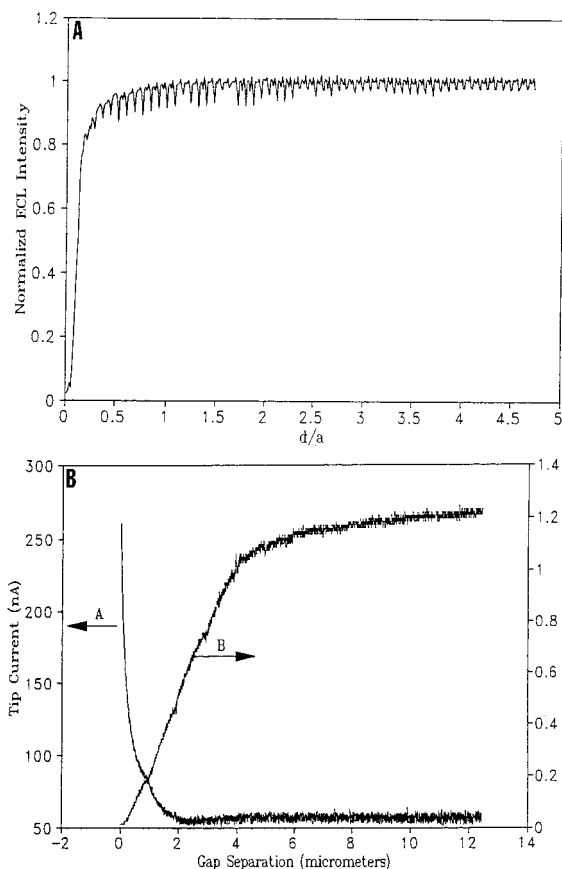
than 0.5 ms, but deviated from this relation when τ was below 0.5 ms. Triple-step ECL experiments[2] have previously shown that the total photonic emission rate (einsteins/s), I, can be evaluated from the faradaic charge passed in the forward step, Q_f, the Coulombic efficiency, ϕ_c, and the pulse width:

$$I = (Q_f\phi_c/F)(1/2\tau) \qquad (2)$$

where F is the Faraday constant. For a coplanar microdisk electrode, Q_f is given by

$$Q_f = 4nFC^b aD(\tau + 2a(\tau/\pi D)^{1/2}) \qquad (3)$$

where n is the number of electrons involved in the redox reaction, C^b is the bulk concentration, and D is the diffusion coefficient of the redox species. Combination of eqs 2 and 3 gives

$$I = 2naDC^b\phi_c(1 + 2a/(\pi Dt)^{1/2}) \qquad (4)$$

Thus, ECL intensity is expected to increase linearly with the concentration of the luminescent species and quadratically with the tip radius and with the inverse square root of τ as observed experimentally when $\tau > 0.5$ ms. However, deviation from this relation occurs at very short τ, probably because of interference from double-layer charging.

SECM Distance Dependence of ECL Intensity over an Insulator. The ECL intensity with the tip close to a substrate will be different from that in bulk solution because of hindered diffusion and feedback effects. Figure 4A shows an ECL approach curve, i.e., the ECL intensity as a function of distance between the tip and an insulating substrate (quartz). An alternating frequency of 50 Hz, which is greater than the bandwidth of the light-measuring circuit, was used to achieve an almost steady (average) ECL level. As shown in this figure, the ECL intensity was nearly steady as the tip approached the quartz substrate until it was a few tenths of the tip radius away from the surface. The ECL intensity then dropped sharply to nearly zero as the tip moved even closer to the surface. This behavior is quite different from that of the i_T vs d curve normally observed in SECM for an insulating substrate. In the latter, the tip current at a constant tip bias decreases smoothly over a distance of a few tip radii before the tip reaches the substrate surface. This kind of sharp distance dependency was also observed for the average tip current produced in an alternating-pulse experiment (as discussed below).

SECM Distance Dependence of Tip Current and ECL Intensity over a Conductor. In this experiment, multiple cycles of alternating potential pulses ($\tau = 10$ ms) between 1.6 and −1.4 V vs SSCE were continuously applied to the tip while it approached or moved away from the surface of an ITO substrate. Both ECL and i_T were sampled at $t_s = 0.95\tau$, i.e., just before the end of each anodic pulse. The reproducible wave forms of ECL intensity and i_T (Figure 3) make this sampling technique useful in obtaining average (quasi-steady-state) ECL and i_T outputs. As shown in Figure 4B, both ECL and i_T remained nearly steady as the tip approached the ITO substrate until it was ~4 μm (~0.3a) away from the ITO surface. ECL intensity then decreased almost linearly while i_T increased inversely with d. Although exact

Figure 4. (A) ECL intensity as a function of the distance between tip (Pt disk, $a = 12.5\ \mu$m) and an insulating substrate (quartz) in MeCN containing 1 mM Ru(bpy)$_3^{2+}$ and 0.2 M TBA-BF$_4$ as the supporting electrolyte. E_T was pulsed between 1.60 and -1.40 V vs SSCE at 50 Hz. (B) Distance dependence of tip current (curve A) and ECL intensity (curve B) over a conducting substrate (ITO) in an MeCN solution containing 1 mM Ru(bpy)$_3^{2+}$ and 0.2 M TBA-BF$_4$. E_T was pulsed between 1.60 and -1.40 V vs SSCE at 50 Hz ($\tau = 10$ ms). Both ECL intensity and tip current were sampled at $t_s = 0.95\tau$ (i.e., just before the end of each anodic pulse). Tip radius $a = 12.5\ \mu$m.

mathematical descriptions of these experimentally observed ECL intensity and i_T vs d curves are still not established, qualitative rationalization of their shapes is possible by comparing the pulse width τ with the diffusional transit time, t_d, expressed as d^2/D. The ECL reaction depends on the annihilation reaction, eq 1, occurring in a reaction zone near the tip electrode. For a given τ, this zone has a thickness of about $(2D\tau)^{1/2}$. As long as this thickness is small compared to d, the tip will not sense or be appreciably perturbed by the presence of the substrate. At a distance where $d^2/2D$ is larger than τ, i_T and ECL intensity are dominated by the diffusion layer developed at the tip during the time of the potential transient. Over this distance range, the ECL intensity and i_T depend mainly on τ and are essentially distance-independent. Conversely, when d is so small that $d^2/2D$ is smaller than τ, the effect of the substrate on the response becomes important. The ECL intensity and tip current in this distance range will depend strongly on d with the transition from one regime to the other regime occurring at a distance near $(2D\tau)^{1/2}$, which is $\sim$5 μm for $\tau = 10$ ms and $D = 1.2 \times 10^{-5}$ cm^2/s. Figure 4B shows that this estimate appears valid.

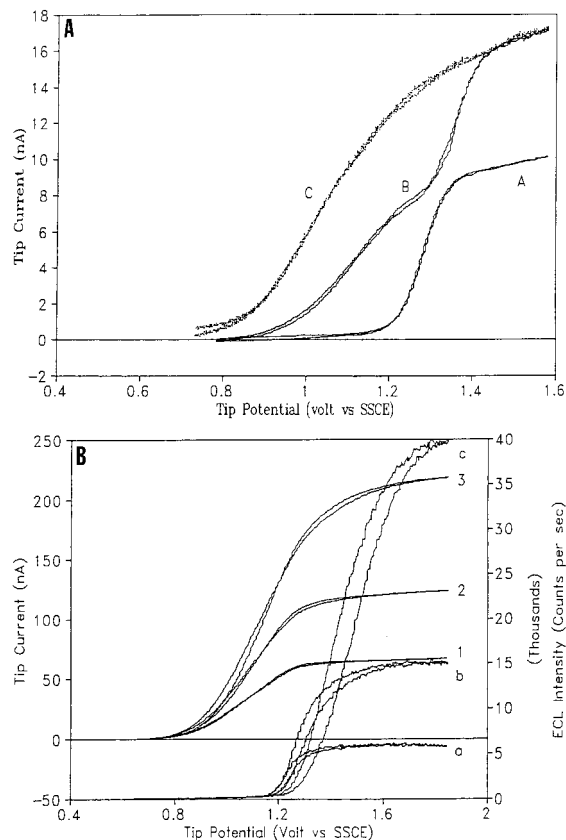**Electrochemistry and ECL Generated by Co-Oxidation of Ru(bpy)$_3^{2+}$ and Tripropylamine at Constant Potential Bias.**

Figure 5. (A) Cyclic voltammograms of (curve A) 1 mM Ru(bpy)$_3^{2+}$ in 0.2 M TBA-BF$_4$ MeCN solution at a Pt microdisk electrode ($a = 12.5\ \mu$m), (curve B) after addition of 0.5 mM TPrA to the solution in (A), and (curve C) in a 1 mM TPrA/0.2 M TBA-BF$_4$ MeCN solution. Scan rate, 5 mV/s. (B) Cyclic voltammograms at a Pt microdisk electrode ($a = 12.5\ \mu$m) in MeCN solutions containing 1 mM Ru-(bpy)$_3^{2+}$, 0.2 M TBA-BF$_4$ as the supporting electrolyte, and (curve 1) 3.5, (curve 2) 6.5, and (curve 3) 12 mM TPrA. The corresponding ECL intensity vs potential curves are shown for (a) 3.5, (b) 6.5, and (c) 12 mM TPrA.

An alternative method of generating ECL involves the use of a coreactant, e.g., generating Ru(bpy)$_3^{3+}$ in the presence of oxalate or TPrA.[13−15] This allows ECL to be generated at a constant (rather than alternating) potential and permits the use of aqueous solutions.[16] In a 0.2 M TBA-BF$_4$/MeCN solution containing only Ru(bpy)$_3^{2+}$, a wave corresponding to the oxidation of Ru(bpy)$_3^{2+}$ occurs at $E_{1/2} = 1.32$ V vs SSCE (curve A, Figure 5A). The addition of 0.5 mM TPrA to this solution produces a voltammo-gram (curve B) with a new additional wave at $E_{1/2} = 1.10$ V vs SSCE, which is coincident with the oxidation wave observed in a 0.2 M TBA-BF$_4$/MeCN solution containing only 1 mM TPrA (curve C). Thus, the oxidation wave at $E_{1/2} = 1.10$ V vs SSCE corresponds to the direct oxidation of TPrA. The steady-state tip current at large d, $i_{T,\infty}$, suggests that this is an overall two-electron oxidation process (assuming $D = 1.8 \times 10^{-5}$ cm^2/s for TPrA). By scanning the tip potential to where both TPrA and Ru(bpy)$_3^{2+}$ are oxidized, a fairly strong and steady ECL intensity can be observed (Figure 5B) where ECL is produced by the following reaction

(13) Chang, M. M.; Saji, T.; Bard, A. J. *J. Am. Chem. Soc.* **1977**, *99*, 5399.
(14) Nofsinger, J. B.; Danielson, N. D. *Anal. Chem.* **1987**, *59*, 865.
(15) Leland, J. K.; Powell, M. J. *J. Electrochem. Soc.* **1990**, *137*, 3127.
(16) Rubinstein, I.; Bard, A. J. *J. Am. Chem. Soc.* **1981**, *103*, 512.
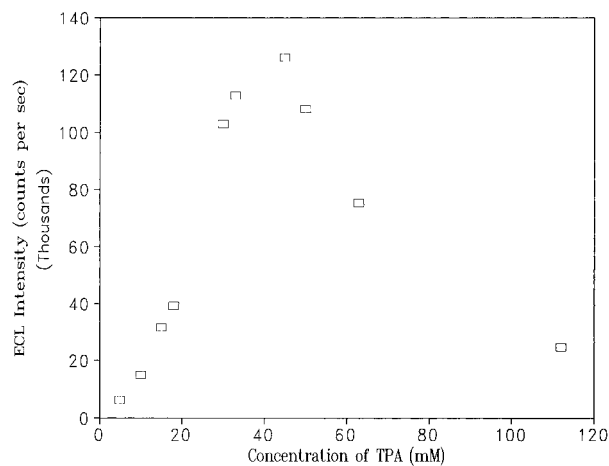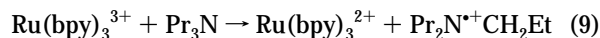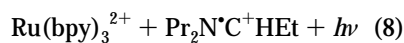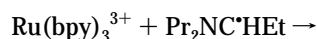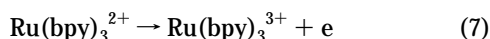
Figure 6. ECL intensity as a function of [TPrA] at $[Ru(bpy)_3^{2+}] = 1$ mM in 0.2 M TBA-BF$_4$ MeCN solution. Each point represents the maximum steady-state value obtained from the ECL intensity vs potential curves for different TPrA concentrations.

scheme.[14,15]

$$Pr_3N \rightarrow Pr_2N^{\bullet+}CH_2Et + e \quad (5)$$

$$Pr_2N^{\bullet+}CH_2Et + Pr_3N \rightarrow Pr_2NC^{\bullet}HEt + Pr_3NH^+ \quad (6)$$

$$Ru(bpy)_3^{2+} \rightarrow Ru(bpy)_3^{3+} + e \quad (7)$$

$$Ru(bpy)_3^{3+} + Pr_2NC^{\bullet}HEt \rightarrow$$
$$Ru(bpy)_3^{2+} + Pr_2N^{\bullet}C^+HEt + h\nu \quad (8)$$

$$Ru(bpy)_3^{3+} + Pr_3N \rightarrow Ru(bpy)_3^{2+} + Pr_2N^{\bullet+}CH_2Et \quad (9)$$

Note that significant ECL intensity is only detected at potentials where $Ru(bpy)_3^{2+}$ is oxidized. The ECL intensity tended to decrease with increasing anodic tip bias after reaching a maximum, while a plateau was usually observed for tip current. This phenomenon became more evident when the concentration of TPrA was high.

In Figure 6, we show the dependence of ECL intensity on the concentration of TPrA at a fixed $[Ru(bpy)_3^{2+}]$. When [TPrA] is <30 mM, the ECL intensity increases as the second power of [TPrA]. This suggests that the generation of each $Ru(bpy)_3^{2+*}$ in this TPrA concentration range involves two TPrA molecules, e.g., via the electron- and proton-transfer reactions indicated by eqs 5, 9, and 6. There is a very small positive intercept for ECL intensity, which we believe represents the trace ECL background we usually observe in a $Ru(bpy)_3^{2+}$ solution containing no intentionally added coreactant. When [TPrA] increases, ECL intensity increases to a maximum at [TPrA] $\approx$ 45 mM and then decreases, following a $[TPrA]^{-1}$ relation. This ECL quenching might be caused by a too complete consumption of $Ru(bpy)_3^{3+}$ by TPrA through reaction 9 decreasing the $Ru(bpy)_3^{3+}$ available in reaction 8. The deactivation of the electrode surface by film formation, as discussed below, is also possible.

SECM with Coreactant. For a 25-μm-diameter tip held 43 μm over a quartz substrate, the ECL intensity at constant tip bias (2.1 V vs SSCE) decayed from ~0.2 μA (photocurrent) to a

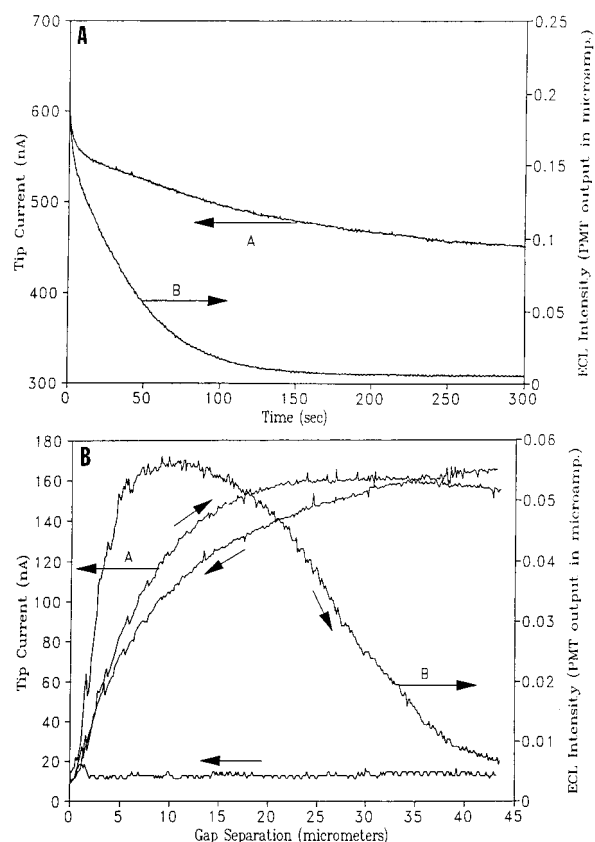**Figure 7.** (A) Time evolution of ECL intensity and tip current after applying a tip potential of 2.1 V vs SSCE. The tip ($a = 12.5 \mu$m) was positioned ~43 μm away from a quartz substrate. The solution contained 1 mM Ru(bpy)$_3^{2+}$, 60 mM TPrA, and 0.2 M TBA-BF$_4$ in MeCN. (B) Approach curves of ECL intensity (curve B) and tip current (curve A) for a tip ($a = 12.5 \mu$m) over a quartz substrate in an MeCN solution containing 1 mM Ru(bpy)$_3^{2+}$, 60 mM TPrA, and 0.2 M TBA-BF$_4$. The tip was biased at 2.1 V vs SSCE.

negligible level (<0.01 μA) within 3 min (Figure 7A). However, the tip current remained at a significant and nearly-steady-state value after the initial rapid decay, presumably due to the depletion of [TPrA]. Since i_T, with the large excess of TPrA as compared with $Ru(bpy)_3^{2+}$, is mainly due to the oxidation of TPrA, while the ECL intensity depends on both [TPrA] and $[Ru(bpy)_3^{2+}]$ near the tip surface, the different decay behavior of ECL intensity and tip current suggests that the tip surface is deactivated and that TPrA and $Ru(bpy)_3^{2+}$ have different accessibilities to the deactivated tip surface. Formation of a thin film on the tip surface at high [TPrA] during TPrA oxidation is probably responsible for tip deactivation. To test this proposal, we carried out a simple experiment by bringing the tip into physical contact with the quartz substrate and then retracting the tip from the quartz surface, with the idea that the initially formed film would be partially broken by the tip touching the quartz surface but then form again during tip retraction.

Figure 7B shows the results of such an experiment, where the tip, positioned 43 μm away from the quartz surface, was biased at 2.1 V vs SSCE. After the ECL intensity decayed to a negligible value (<0.005 μA), the tip was moved slowly toward the substrate until i_T dropped nearly to zero (~2 orders of magnitude smaller than $i_{T,\infty}$). The tip was then withdrawn back to the starting position. As seen in this figure, when the tip approached the
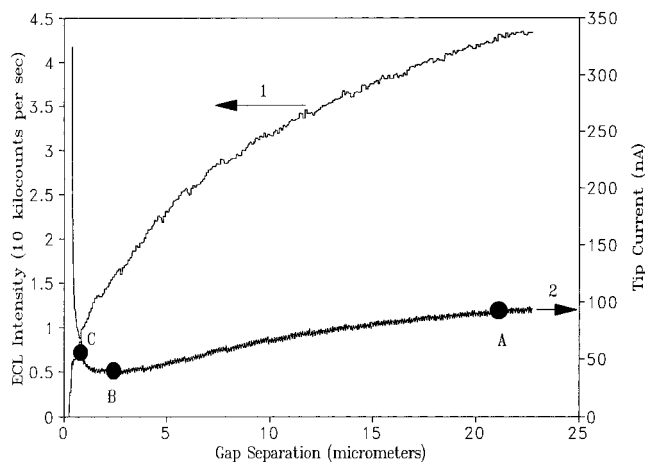
Figure 8. Distance dependence of ECL intensity (curve 1) and tip current (curve 2) over a conducting substrate (ITO) in an MeCN solution containing 1 mM $Ru(bpy)_3^{2+}$, 20 mM TPrA, and 0.2 M TBA-BF_4 as the supporting electrolyte. The tip ($a = 12.5\ \mu m$) was biased at 2.1 V vs SSCE and the substrate at -0.30 V vs SSCE.

quartz substrate, the ECL intensity stayed constant and small while the tip current decreased with decreasing d, as expected. When the tip was withdrawn after touching, the tip current was nearly retraceable while the ECL intensity showed a strong increase. We tentatively attribute the initial large increase in ECL intensity to a refreshing of part of the deactivated electrode surface, which allowed for more oxidation of $Ru(bpy)_3^{2+}$ and thus more intense ECL. The decay of ECL intensity following the initial increase then indicates reformation of a thin film which blocks the reaction of $Ru(bpy)_3^{2+}$ at the tip surface.

In the previous section, we described the behavior of SECM and ECL intensity over an insulating substrate. We showed that, under those conditions, ECL intensity at constant tip bias decayed with time to reach a very small level. However, at the same tip bias, the stability of ECL intensity can be dramatically enhanced over a conducting substrate, like ITO, if the tip is not too far away from the substrate. This allows a study of the distance dependence of i_T and ECL intensity. In Figure 8, the tip is biased at 2.1 V vs SSCE to oxidize both TPrA and $Ru(bpy)_3^{2+}$, and ECL intensity decreased monotonically as the tip approached the ITO surface. However, i_T decreased to a minimum and then increased as the tip came even closer before showing a very sharp increase, presumably because of electron tunneling between tip and ITO. This type of current vs distance relation has usually been attributed to the effect of homogeneous kinetics on the electrontransfer reactions.[17-19] To elucidate the mechanisms responsible for this approach behavior, we carried out several experiments. Figure 9A shows three cyclic voltammograms taken at three different distances, specified as points A, B, and C on the i_T vs d curve shown in Figure 8. The amplitude of the wave corresponding to the oxidation of TPrA only ($E_{1/2} = 1.1$ V vs SSCE) was found to decrease monotonically with decreasing d. This result is consistent with the i_T vs d curve taken at $E_T = 1.2$ V vs SSCE (where only TPrA is oxidized) as shown in Figure 9B. The oxidation of TPrA and its associated irreversible homogeneous
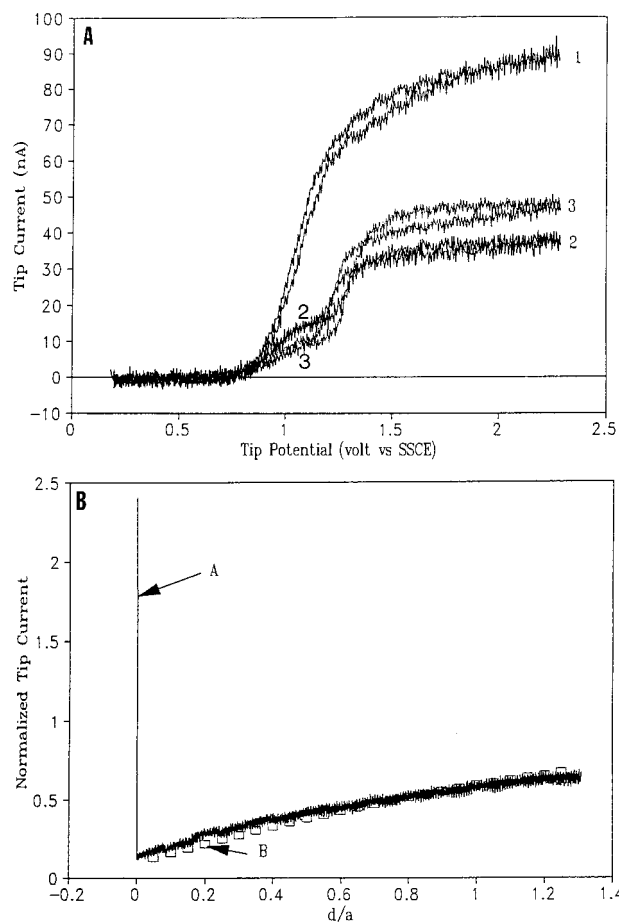
(17) Unwin, P. R.; Bard, A. J. *J. Phys. Chem.* **1991**, *95*, 7814.
(18) Treichel, D. A.; Mirkin, M. V.; Bard, A. J. *J. Phys. Chem.* **1994**, *98*, 5751.
(19) Zhou, F.; Bard, A. J. *J. Am. Chem. Soc.* **1994**, *116*, 393.

Figure 9. (A) Cyclic voltammograms on a Pt disk ($a = 12.5\ \mu m$) taken at three different distances over an ITO substrate, specified as points A (curve 1), B (curve 2), and C (curve 3) on the i_T vs d curve shown in Figure 8. The substrate was biased at -0.30 V vs SSCE and scan rate was 5 mV/s. (B) Tip current approach curves at $E_T = 1.20$ V and $E_S = -0.30$ V vs SSCE. Curve A (line), experimental data; curve B (squares), simulated curve for insulating substrate. The solution was the same as used in Figure 8.
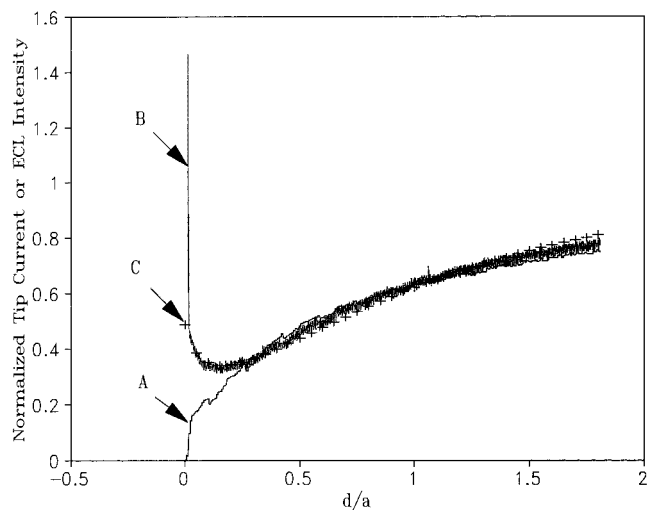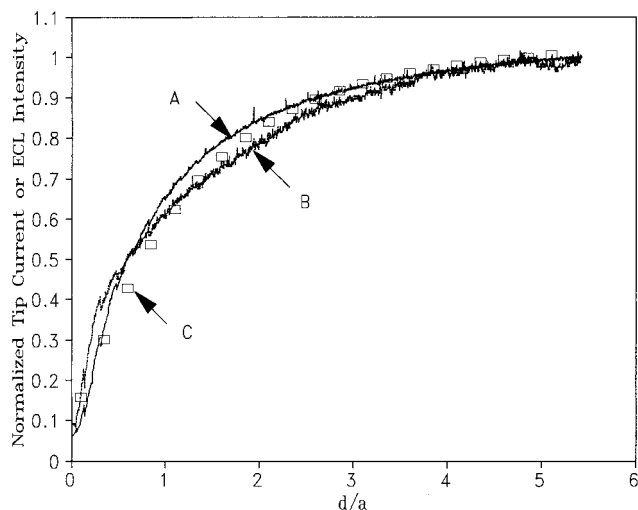

Figure 10. (A) Experimental normalized ECL intensity vs normalized distance for data taken from curve 1 of Figure 8. (B) Experimental normalized tip current vs normalized distance for data taken from curve 2 of Figure 8. (C) (pluses), simulated normalized tip current vs normalized distance based on a 95% contribution from the irreversible oxidation of TPrA and a 5% contribution from the reversible oxidation of $Ru(bpy)_3^{2+}$.

Figure 11. Distance dependence of tip current (curve A) and ECL intensity (curve B) over a quartz substrate in an MeCN solution containing 1 mM Ru(bpy)$_3^{2+}$, 20 mM TPrA, and 0.2 M TBA-BF$_4$. Curve C (squares), simulated SECM approach curve for an insulating substrate.

reactions alone is not responsible for the approach behavior shown in Figure 8. A more reasonable mechanism involves a combination of the positive feedback of Ru(bpy)$_3^{2+}$ oxidation, the regeneration of Ru(bpy)$_3^{2+}$ by TPrA, and the negative feedback of TPrA oxidation due to the irreversibility of its oxidation. Figure 10 shows a theoretical i_T vs d curve based on a 95% contribution from the irreversible oxidation of TPrA and a 5% contribution from the reversible oxidation of Ru(bpy)$_3^{2+}$. The agreement between experiment and theory is reasonable, although detailed kinetics and mechanisms of the homogeneous reactions between Ru(bpy)$_3^{3+}$ and TPrA are required for a better fit.

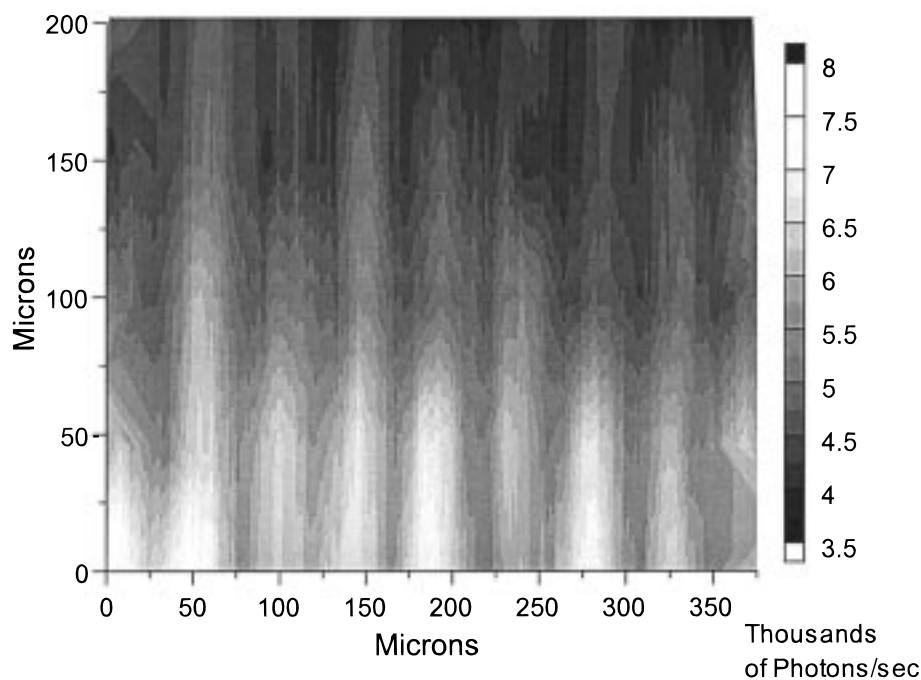**ECL Generated by Co-Oxidation of Ru(bpy)$_3^{2+}$ and TPrA in an Alternating Potential Pulse Mode.** As shown in the previous section, the ECL intensity over an insulating substrate at constant tip bias is not stable enough for imaging purposes. However, the stabilities of both ECL intensity and tip current can be substantially increased by using a pulsed rather than a constant-potential generation mode, presumably because of decreases in the amounts of TPrA-associated intermediates which promote film formation at the tip surface. In this experiment, continuous cycles of alternating potential pulses ($\tau = 10$ ms) between 2.1 and 0.1 V vs SSCE were applied to the tip while ECL intensity and i_T were monitored as functions of time. To obtain a steady ECL intensity and tip current, the same data sampling technique as described previously ($t_s = 0.95\tau$) was used. Both the ECL intensity and tip current were steady and high for at least 10 min, which is sufficient time for taking one frame of an image (128 × 128 pixels) at the usual SECM rastering speed (e.g., 0.5 Hz). The high stabilities in ECL intensity and tip current also make studies of their distance dependence over an insulating substrate possible. As shown in Figure 11, both ECL intensity and tip current decrease monotonically with decreasing distance and follow quite well the theoretical approach curve for the tip current with an insulating substrate.

ECL Tip Imaging. One of the purposes of this experiment was to explore the possibility of using an ECL probe as a small light source for optical imaging. As a demonstration, a preliminary experiment was carried out with an interdigitated array (IDA), which consists of Au bands (30 μm wide) spaced 25 μm apart deposited on a glass substrate. Line scan images with an ECL probe are shown in Figure 12. For this image a Pt disk (5 μm diameter) operating in the annihilation mode served as the tip. It was immersed in an ambient-exposed MeCN solution containing 15 mM Ru(bpy)$_3^{2+}$ and 0.21 M TBA-BF$_4$ as the supporting electrolyte. The tip was pulsed at 8 kHz between potentials where Ru(bpy)$_3^{3+}$ and Ru(bpy)$_3^+$ were sequentially generated at the tip. The IDA structure served as the bottom of a Teflon electrochemical cell and was clamped to the cell through an O-ring. The image

Figure 12. Raw SECM/ECL image of an interdigitated array structure which consists of Au bands (30 μm wide) spaced 25 μm apart deposited on a glass substrate. A Pt disk tip (5-μm diameter) in an MeCN solution containing 15 mM Ru(bpy)$_3^{2+}$ and 0.21 M TBA-BF$_4$ was pulsed at 8 kHz to generate Ru(bpy)$_3^{3+}$ and Ru(bpy)$_3^+$.

was obtained by scanning the tip at a constant height in the $x-y$ plane and detecting the ECL intensity with a PMT located beneath the sample. For this sample, the ECL intensity detected by the PMT reflects mainly the local absorbance of the substrate. However, contrast mechanisms based on the chemical or topographical nature of the substrate should also be possible and are now under investigation.

CONCLUSIONS

The generation of ECL at a tip in the SECM can be carried out either by ion annihilation or with a coreactant. Modes of operation that produce sufficiently intense and stable ECL for optical imaging are possible. The SECM/ECL approach curves (intensity vs tip−substrate distance, d) with both insulating and conducting substrates show a decreased ECL intensity with a decrease in d. Measurement of the tip current at the same time the ECL is measured is convenient for determination of d in optical scanning experiments.

The demonstrated resolution in optical imaging experiments for this technique is only in the micrometer range. Improved resolution to obtain the 100-nm resolution that is possible with laser illumination through quartz capillaries in NSOM will require smaller tips and spacing in the near-field region. As shown in this study, this presents challenges in terms of the light intensities that can be generated in close proximity to a surface. In the annihilation mode, high frequencies will be required to produce a reaction layer sufficiently close to the electrode surface to prevent reactants from diffusing away from one another. Kinetics may also be a problem in coreactant schemes. However, investigation of ECL with the SECM may be useful in elucidating the kinetics and mechanisms of coreactant ECL reactions, which have been difficult to study by conventional electrochemical methods.